ORNL/TM-2014/141

Performance Evaluation of Advanced Retrofit Roof Technologies Using Field-Test Data – Phase Three Final Report, Volume 1

May, 2014

Prepared by
Kaushik Biswas, Ph.D.
Phillip Childs
Jerald Atchley

ORNL/TM-2014/141

Energy and Transportation Science Division

Performance Evaluation of Advanced Retrofit Roof Technologies Using Field-Test Data – Phase Three Final Report, Volume 1

Kaushik Biswas
Phillip Childs
Jerald Atchley

Date Published: May, 2014

Prepared by
OAK RIDGE NATIONAL LABORATORY
Oak Ridge, Tennessee 37831-6283
managed by
UT-BATTELLE, LLC
for the
U.S. DEPARTMENT OF ENERGY
under contract DE-AC05-00OR227

TABLE OF CONTENTS

ABSTRACT

This article presents various metal roof configurations that were tested at Oak Ridge National Laboratory in Tennessee, U.S.A. between 2009 and 2013, and describes their potential for reducing the attic-generated space conditioning loads. These roofs contained different combinations of phase change material, rigid insulation, low emittance surface and above-sheathing ventilation, with standing-seam metal panels on top. These roofs were designed to be installed on existing roofs decks, or on top of asphalt shingles for retrofit construction.

All the tested roofs showed the potential for substantial energy savings compared to an asphalt shingle roof, which was used as a control for comparison. The roofs were constructed on a series of adjacent attics separated at the gables using 6 inch thick foam insulation. The attics were built on top of a conditioned room. All attics were vented at the soffit and ridge. The test roofs and attics were instrumented with an array of thermocouples. Heat flux transducers were installed in the roof deck and attic floor (ceiling) to measure the heat flows through the roof and between the attic and conditioned space below. Temperature and heat flux data were collected during the heating, cooling and 'swing' seasons over the test period. Data from previous years of testing have been published. Here, data from the latest roof configurations being tested in phase 3 of the project (May 2012 – December 2013) are presented. All test roofs were highly effective in reducing the heat flows through the roof and ceiling, and in reducing the diurnal attic temperature fluctuations.

INTRODUCTION

This article describes phase 3 of a study that began in 2009 to evaluate the energy benefits of a sustainable re-roofing technology utilizing standing-seam metal roofing panels combined with energy efficient features like above-sheathing-ventilation (ASV), phase change material (PCM) and rigid insulation board. The data from phases 1 and 2 have been previously published and reported [Kosny et al., 2011; Biswas et al., 2011; Biswas and Childs, 2012; Kosny et al., 2012]. Based on previous data analysis and discussions within the research group, additional test roofs were installed in May 2012, to test new configurations and further investigate different components of the dynamic insulation systems.

It has been well-documented that roofs and attics experience higher temperature fluctuations than other building envelope components. A study by Huang et al. [1999] found roofs contributed 12-14% of the heating and cooling loads in residential buildings. A great deal of research work has been devoted to reducing the roof and attic generated space conditioning loads. Parker et al. [1995] compared the heat transfer through direct-nailed and counter-batten tile roofs to an asphalt shingle roof and found 50 percent reductions in heat transfer. Akbari et al. [2004] found that a roof surface with high solar reflectance and high thermal emittance resulted in cooling energy savings in moderate and hot climates. Miller and Kosny [2007] studied prototype roof designs that combined strategies like infrared reflective roofs, radiant barriers, ASV, low emittance (low-e) surfaces, insulation and thermal mass to regulate the attic temperature and reduce the ceiling heat transfer. Attic radiant barriers have shown the potential for reducing radiation heat exchange across roof cavities and attic spaces [Medina, 2010]. In addition to the aforementioned technologies, PCMs are increasingly being investigated for use in building envelopes,

including roofs, for thermal storage and a consequent reduction in space conditioning loads. Zalba et al. [2003], Sharma et al. [2009] and Xin et al. [2009] have provided detailed reviews of the thermal storage systems incorporating PCMs, including those for building envelope applications.

The current test roofs combined PCM, fiberglass insulation, a low emittance (low-e) surface and above-sheathing-ventilation in different configurations to evaluate their potential in reducing the heating and cooling loads in buildings. In addition to the steady thermal resistance of the fiberglass insulation, these roofs utilize the dynamic effects of the PCM, ASV airflow and the low-e surface to reduce the heat flow through the roof. The roofs were designed and built by a collaboration between Metal Construction Association (MCA), CertainTeed Corporation, Phase Change Energy Solutions and Oak Ridge National Laboratory (ORNL). MCA is a North American trade association of metal building manufacturers, builders, and material suppliers; CertainTeed is a manufacturer of thermal insulation and building envelope materials; and Phase Change Energy Solutions manufactured the PCM.

The current dynamic roofs were designed such that they can be installed in new construction or on top of existing roofs. According to a 2002 report [Dodge, 2002], asphalt shingles covered more than 85% of the residential roofing area in the United States (U.S.). Re-roofing at the end of their service lives generates an estimated 6.8 million tons of waste asphalt shingles per year in the U.S., requiring large disposal areas [Sengoz and Topal, 2005]. Using the present dynamic roofing systems for re-roofing and retrofitting applications precludes the asphalt shingle waste generation, in addition to improving the energy efficiency of the building.

DESCRIPTION OF TEST ROOFS

These test roofs were built on side-by-side attics on the Envelope Systems Research Apparatus (ESRA) facility in Oak Ridge, TN. The attics are thermally isolated from each other by using foam insulation at the gable ends and are vented at the soffit and ridge. A conventional asphalt shingle roof was used as a control to evaluate the energy benefits of the test roofs. Further details of the attic construction are provided by Miller [2006].

Figure 1 shows the attic roofs located on the ESRA facility. Three test roofs are described in this article and will be referred to as: ‘Lane 2 – ASV HG’, ‘Lane 3 – PCM’, ‘Lane 4 – PCM ASV’ and ‘Lane 5 – Poly PV’. ‘Lane 6 – Shingle’ is the control roof built with asphalt shingles on the roof deck [Kosny et al., 2012]. The test roofs were constructed with different configurations of rigid fiberglass insulation, PCM, air gap (ASV) under the metal panels, and polycyrstalline photovoltaic panels (lane 5), as shown in Figure 2. Figure 2 also shows how the roof assemblies were instrumented to measure the temperature distribution and heat flow through the oriented strand board (OSB) deck into and out of the attic.

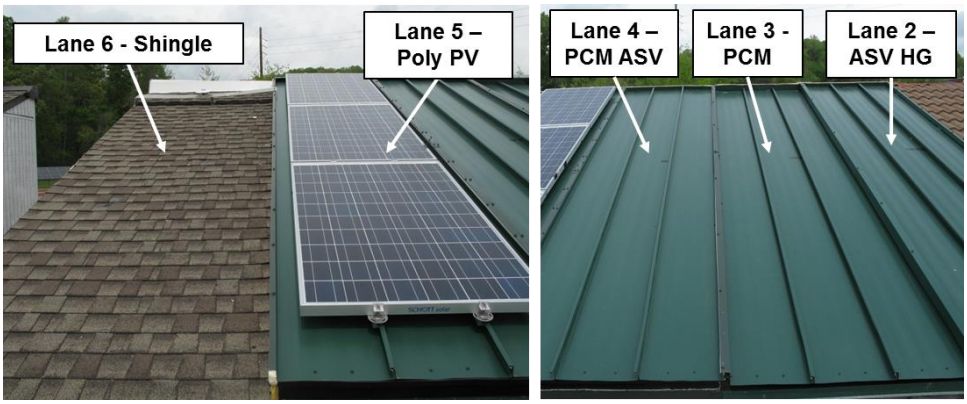

Figure 1. Control asphalt shingle roof (left) and the test roofs (right).

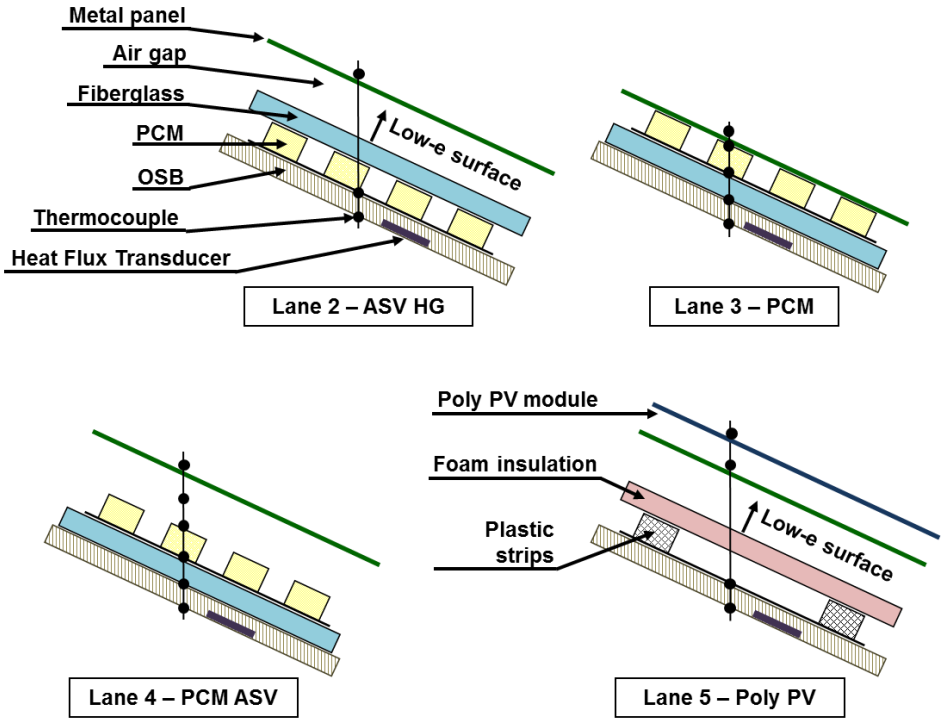

Figure 2. Test roof configuration schematics.

Lane 5 consisted of plastic strips placed on top of the oriented strand board (OSB) roof deck followed by a layer of 1.3 cm thick (R_{SI} – 0.56 m^2·K/W, R_{US}-3.2 hr-ft^2-°F/Btu) polyisocyanurate foam insulation with a reflective low-emittance (low-e) surface facing the sky, and standing seam metal panels on top. The metal panels were supported by metal sub-purlins that provided a 2-inch air gap over the foam insulation for above-sheathing-ventilation (ASV); the air gap was vented both at the ridge and the eave. Finally, polycrystalline PV modules were attached to the metal panels. The configuration of the roof was identical to the 'PV roof' during phase two of this study [Biswas and Childs, 2012], except the laminated PV modules were replaced by the offset-mounted polycrystalling PV modules.

Lane 4 consisted of rigid fiberglass insulation on the OSB roof deck, followed by a layer of macro-encapsulated bio-based PCM and the standing-seam metal panels on top. The metal panels were placed on top of metal sub-purlins that provided an air gap of about 5.1 cm over the PCM layer; the air gap was vented both at the ridge and the eave providing above-sheathing-ventilation (ASV) [Miller and Kosny, 2007]. The fiberglass insulation is about 2.5 cm thick and has a thermal resistance of 0.76 m^2·K/W (4.3 ft^2·hr·°F/Btu). The PCM was packed in arrays of plastic cells of dimensions 4.4 cm x 4.4 cm x 1.3 cm with 1.3 cm spacing (air pockets in plastic cells represented about 20% of the total volume). The nominal heat storage capacity of the PCM packed in the plastic film pouches is about 560 kJ/m^2 of the roof area. The PCM has nominal melting and freezing temperatures of about 30°C and 26°C, respectively. The melting phase transition enthalpy of the PCM is about 190 J/g.

Lane 3 was constructed with the same rigid fiberglass insulation on the roof deck, followed by the PCM layer, but did not contain any air gap above the PCM layer. It should be noted that the 1.3 cm spacing between the air channels still provided some above-sheathing-ventilation in this roof.

The fiberglass board in lane 2 contained a reflective foil facing that introduces a low-e surface which acts to reflect the incoming solar radiation and helps reduce daytime cooling loads. This roof was similar to the one studied during phase 1 of this project [Biswas et al., 2011; Kosny et al., 2012], except for the absence of laminated photovoltaics. In addition to the thermocouples shown in Figure 2, lane 2 was instrumented with two thermocouples each in the air gap close to the ridge and the eave sections. The intent was to try and quantify the heat gain in the buoyant air flow generated in the air gap by natural convection (hence the nomenclature ‘ASV HG’).

ATTIC CONSTRUCTION AND INSTRUMENTATION

Figure 3 shows the typical attic construction and instrumentation on the ESRA facility. The attics are built on top of a conditioned basement. The basic roof construction consists of a weather barrier (moisture shield) on top of a 1.6 cm OSB deck. The asphalt shingles (in lane 6, the control roof) or other test roof components are installed on top of the roof deck. The attic floor or ceiling consists of two wooden fiberboards on top of a corrugated metal sheet. No ceiling insulation was used in this study. However, during phase 1 of this study, R-6.7 m^2·K/W (38 ft^2·hr·°F/Btu) ceiling insulation was installed in all attics [Biswas et al., 2011; Kosny et al., 2012]. In phase 3, the ceiling insulation was removed to check the energy-saving impact of the prototype roofs in retrofit applications where the original attic is poorly insulated or missing insulation.

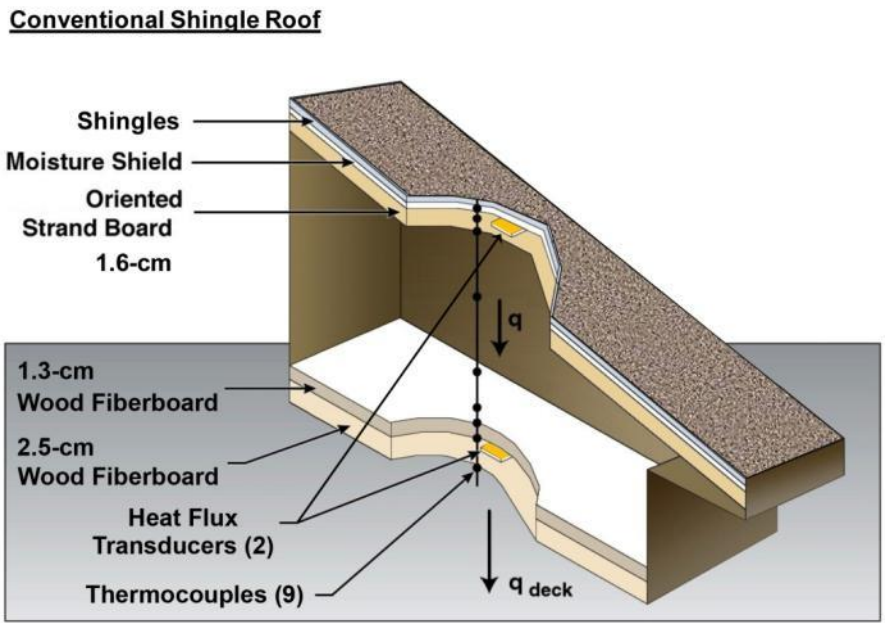

Figure 3. Typical ESRA attic instrumentation

Type T copper-constantan thermocouples are placed within the attic, roof assembly and the ceiling, as shown in Figure 3. These are in addition to the thermocouples shown in Figure 2 and the ones added to the ASV air gap in lane 2. Heat flux transducers (HFT), with an accuracy of ±5% and a sensitivity of 5.7 $(W/m^2)/mV$, measure the heat flows through the ceiling and the roof deck. The HFTs were calibrated using a heat flow meter apparatus while sandwiched by the same materials as in the roof deck and the ceiling, respectively. The heat flow towards the conditioned space is defined as positive (heat flow into the attic from the roof and heat flow into the conditioned basement from the attic), and vice versa.

In addition to the attic instrumentation, an on-site weather station is installed that measures the solar irradiance on the sloped roofs, long wave radiation beyond 3 micrometers (μm), ambient dry bulb temperature, ambient air relative humidity, etc.

RESULTS AND DISCUSSION

In the following sections, data from the test attics are presented and discussed. The temperature and heat flux data were averaged over 15 minute periods and stored in weekly data files. Here, data collected during summer, fall and winter of 2012-13 are shown. Specifically, the evaluation period extends from May 30, 2012 to January 1, 2013.

Roof Surface Temperatures

Figure 4 shows the temperature variations during 3 summer and 3 winter days. Also shown is the outdoor ambient temperature during those days. The maximum roof surface temperatures rose well

above the outdoor temperature due to the daytime solar irradiance. At night, radiation losses to the sky (especially in the absence of cloud cover) lower the roof temperatures below the ambient. No significant differences were observed in the between lanes 2, 3, and 4, and asphalt shingle roof temperatures. The metal roof surface on lane 5 remained cooler during the daytime during both summer and winter periods, due to the shading effect from the offset-mounted PV modules. The recorded roof surface temperatures of lane 3 (PCM) were lower than the other roofs during the winter days shown in Figure 4(B). It was later discovered that the lane 3 roof thermocouple detached from the roof surface and was measuring the air temperature above the roof. Once fixed, lane 3 roof temperatures were similar to the other roofs.

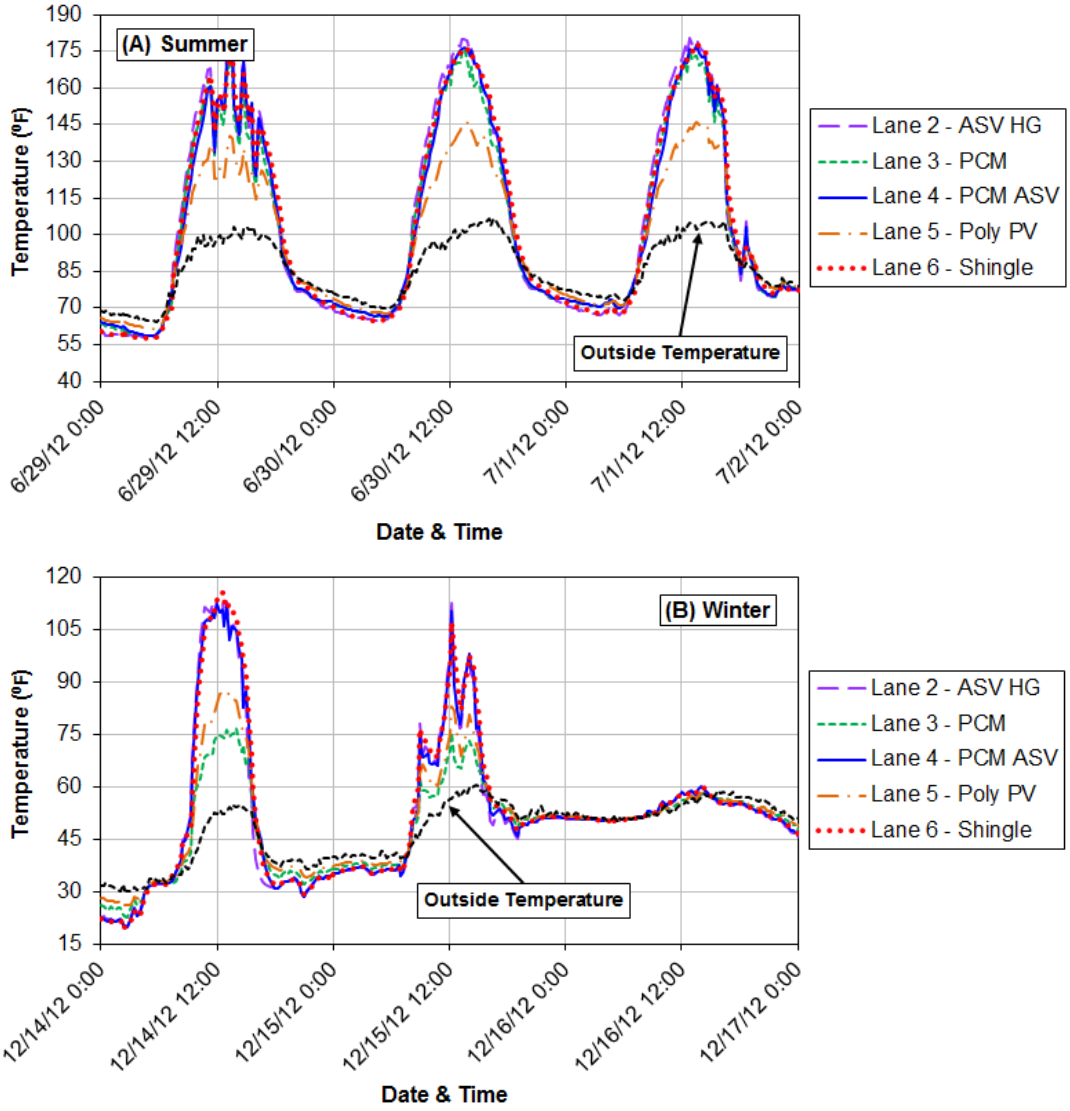

Figure 4. Roof surface temperature variations during: (A) summer and (B) winter.

PCM Behavior

The PCM used in the present experiment was tested using a differential scanning calorimeter (DSC). The phase change characteristics of the PCM are shown in Figure 5. The heating and cooling rate used in the DSC tests was 0.3°C (0.54°F) per minute, and the resulting melting and freezing thresholds were observed to be 25.7°C (78.3°F) and 27.2°C (81.0°F), respectively.

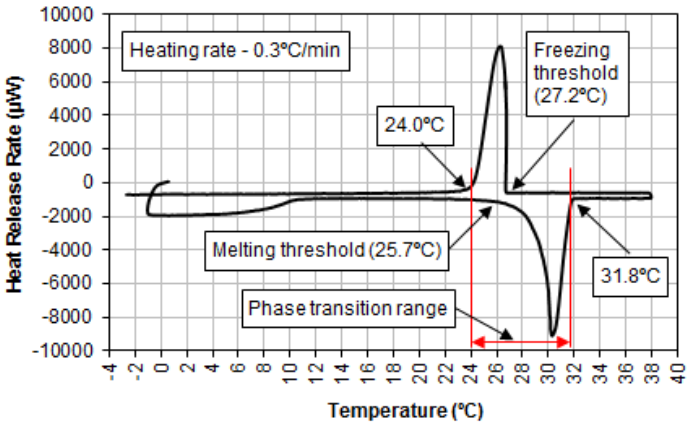

Figure 5. Heat flow data of the PCM from differential scanning calorimetry [Kosny et al., 2012].

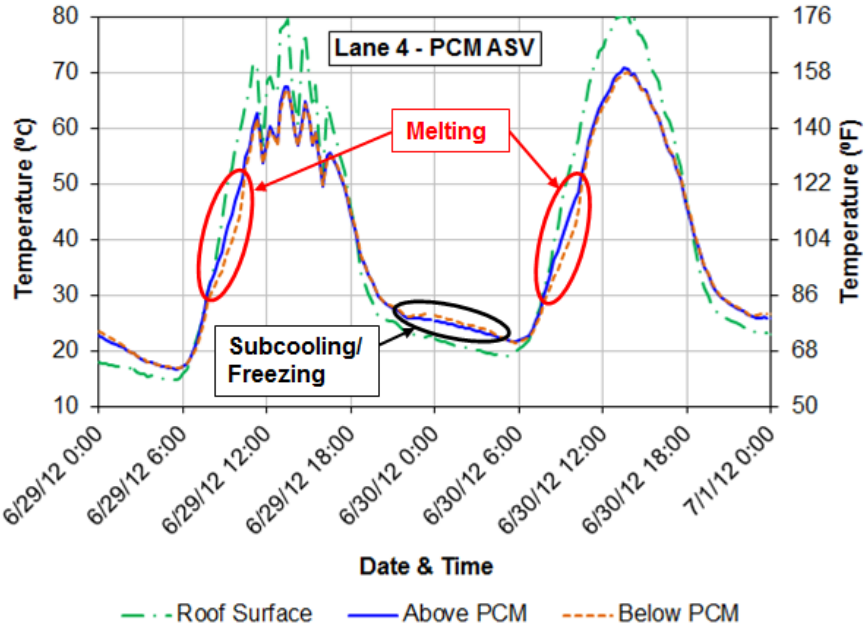

Figure 6. Summer PCM behavior

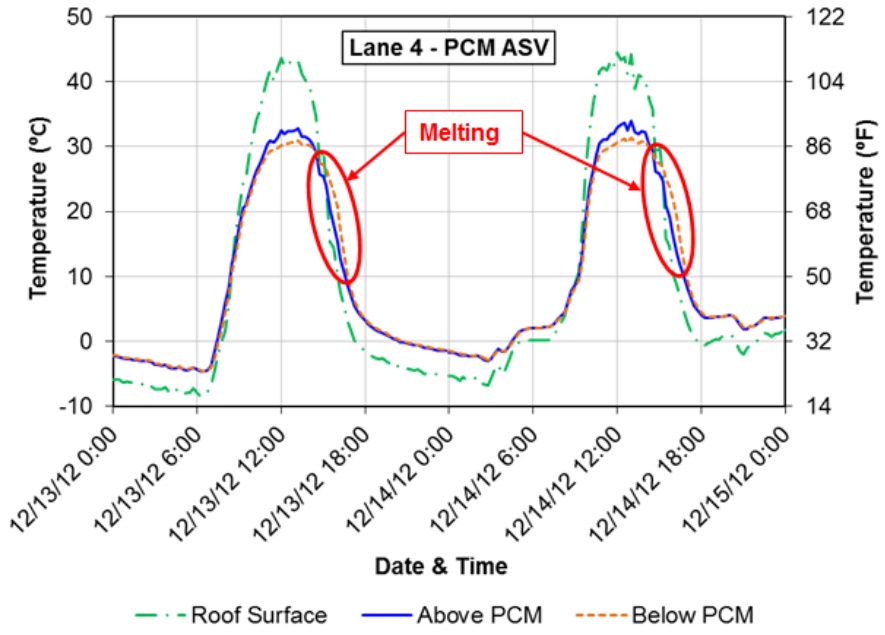

Figure 7. Winter PCM behavior

Figure 6 and Figure 7 show the temperatures above and below the PCM layer during the typical summer and winter days in lane 4. The roof design studied in phase 1 of this project was very effective in regulating the attic temperature and reducing the ceiling heat flows, but temperature data indicated that the PCM remained frozen and was inactive throughout the winter period [Biswas et al., 2011; Kosny et al., 2012]. In the current design of lane 4, the PCM is placed on top of the fiberglass insulation.

As indicated by the temperature separation between the top and bottom of the lane 4 PCM layer in Figure 6 and Figure 7, the PCM did undergo both melting and freezing during both summer and winter periods, as described by Kosny et al. [2012]. Figure 8 shows the weekly maximum and minimum temperatures across the PCM layer in both lane 3 and lane 4 roofs, compared to the phase change onset temperatures from the DSC tests. The weekly minimum temperatures always remained below the freezing threshold temperature, and the maximum temperatures were always above the melting threshold. Thus, on a weekly basis, the PCM in both lanes 3 and 4 can be expected to have been active during both summer and winter periods. It should be noted that DSC heating rate of 0.3°C per minute is higher than the temperature change rates in actual building envelopes. The data shown in Figure 6 and Figure 7 revealed a temperature rise rate of about 0.1°C (0.18°F) per minute at the PCM layer. At lower heating rates, the melting threshold can be expected to be lower than 25.7°C (78.3°F) and the freezing threshold higher than 27.2°C (81.0°F) [Castellón, 2008], making the observed temperatures in lanes 3 and 4 even more conducive to melting and freezing of the PCM.

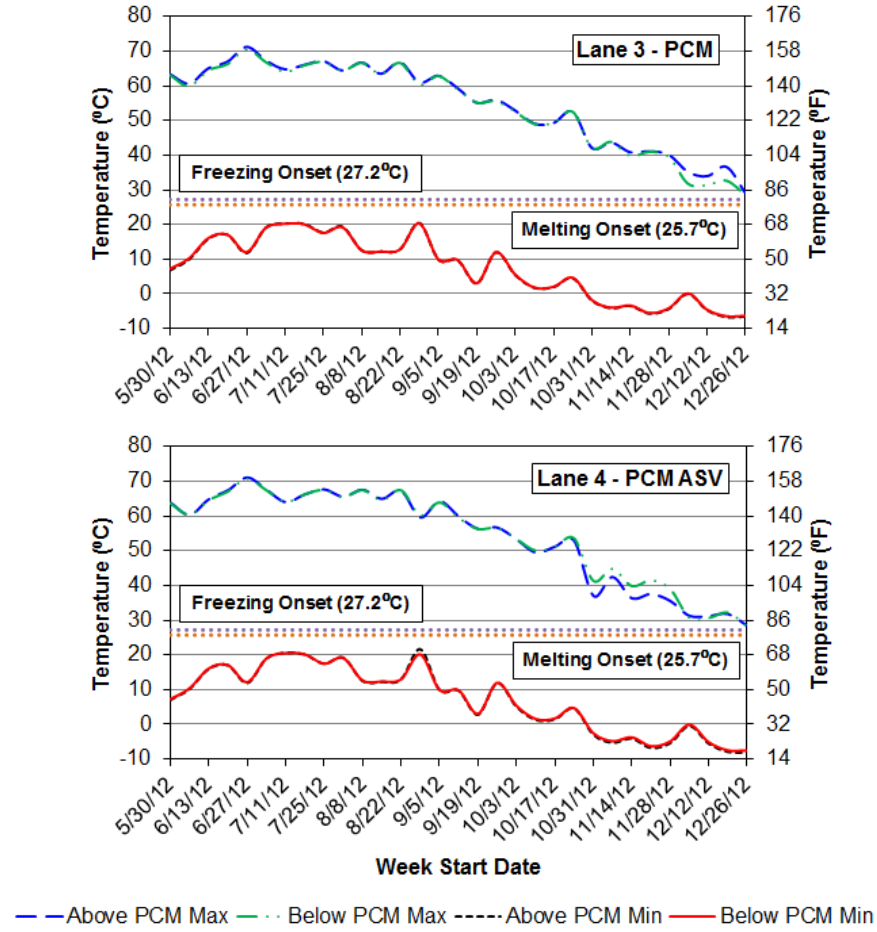

Figure 8. Weekly maximum and minimum PCM surface temperatures

Summer Performance

This section presents temperature and heat flux data from 3-day period during a summer week (June 27 – July 3, 2012), when highest peak outdoor temperatures were observed, and the overall summer period (defined as June 1 – September 30, 2012). Figure 9 shows the variation of the roof heat flux during the summer week. Compared to the control ('shingle' roof), the 'ASV HG' and 'Poly PV' roofs reduced the peak daytime heat gain by about 90% while 'PCM' and 'PCM ASV' roofs reduced the peak heat gain by 80%. The shading effect of the PV modules combined with the foam insulation and ASV in the 'Poly PV' roof led to the significant reductions in roof heat gain. Due to the melting of PCM (and the proximity of the PCM to the roof HFT), on some days, the roof HFT in the 'ASV HG' roof actually showed a reversal of heat flow direction (negative heat flow) during the afternoons.

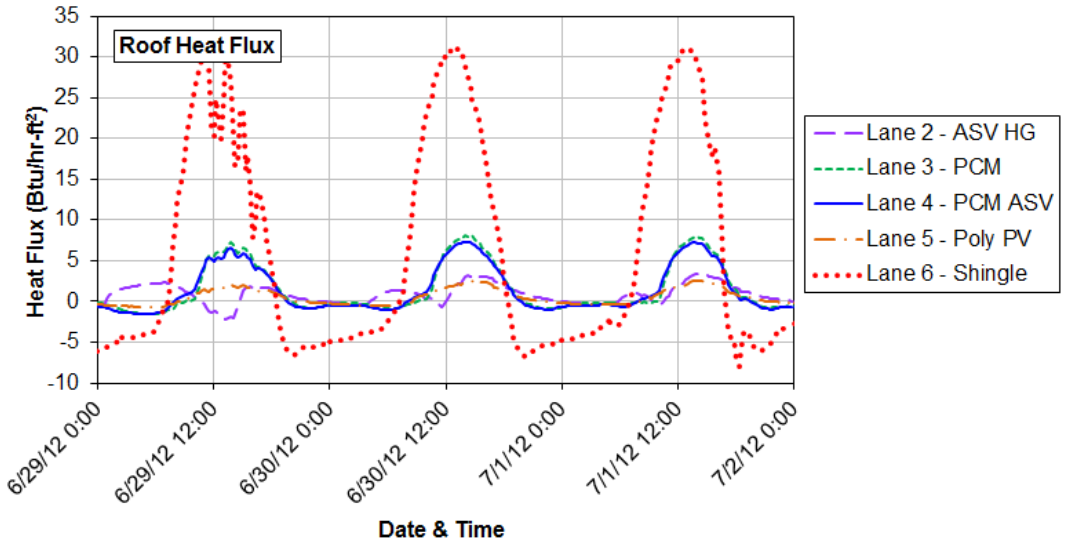

Figure 9. Summer roof heat flux variation

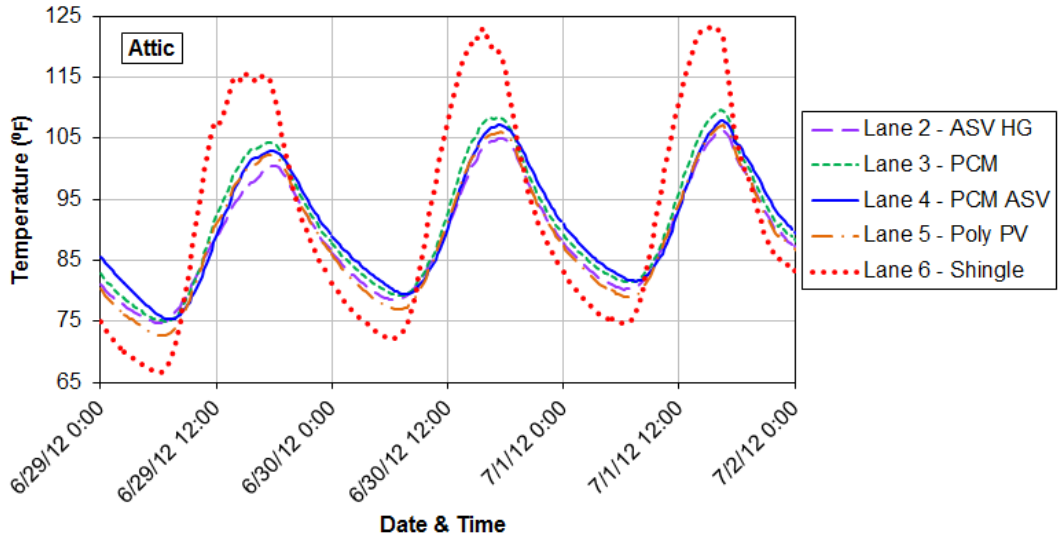

Figure 10. Summer attic temperature variation

Figure 10 shows the attic temperatures during the summer week. All test lanes were effective in lowering the diurnal fluctuations on the attic temperature, and reduced the peak daytime temperatures. The 'ASV HG' attic experienced the lowest peak temperatures, about 17.9°F lower than peak control attic temperatures during this week; the 'PCM', 'PCM-ASV' and 'Poly PV' peak attic temperatures were 13.6°F, 14.9°F and 15.8°F lower than the control.

From a space conditioning perspective, it is most interesting to examine the ceiling heat flux, which directly impacts the heating and cooling loads. Figure 11 shows the weekly ceiling heat flux variations in the different attics. Again, all the test roofs were highly effective in reducing the ceiling heat gains compared to the asphalt shingle roof. During this week, on average, the peak ceiling heat gains in the

different attics were: 'ASV HG' – 2.2 Btu/hr-ft^2, 'PCM' – 2.3 Btu/hr-ft^2, 'PCM ASV' – 2.4 Btu/hr-ft^2, 'Poly PV' – 2.7 Btu/hr-ft^{2}and 'Shingle' – 5.8 Btu/hr-ft^2.

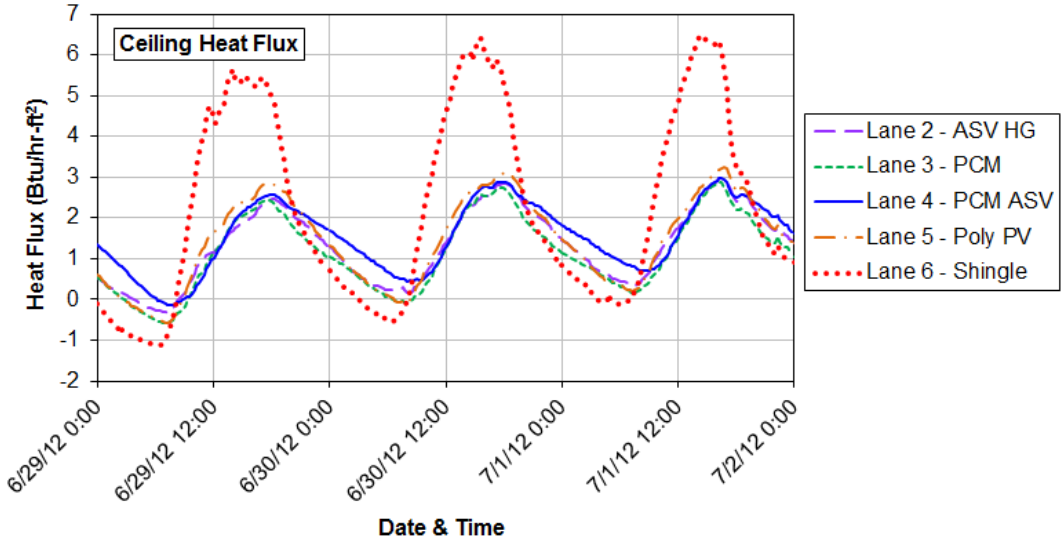

Figure 11. Summer ceiling heat flux variation

To further evaluate the performance of the test roofs over the entire cooling period, the attic temperatures and the ceiling heat flows were averaged over June 1 – September 30, 2012. The averaging (referred to as bin-averaging) was done over corresponding 15-minute periods of each day, and the resulting average data are shown over a 24-hour period in Figure 12 and Figure 13. Bin-averaged outside temperatures are also shown in Figure 12.

The peak averaged-attic temperatures in the test lanes were 89.0°F ('ASV HG'), 93.1°F ('PCM'), 92.5°F ('PCM ASV') and 90.9°F ('Poly PV'), compared to 103.4°F in the asphalt shingle attic. Further, a delay of about 2-2.5 hours was observed in occurrence of the peak temperature in the test attics compared to the asphalt shingle attic, which allows the benefit of peak load shifting for utilities. Further, space conditioning equipment have higher efficiency at lower ambient temperatures which results in less energy usage to meet the loads with the peak shifting. The averaged ceiling heat flows showed a similar trend as the attic temperatures, with a delay of about 2-2.5 hours in the occurrence of the peak ceiling heat flow. The peak ceiling heat flows in the test attics were: 1.1 Btu/hr-ft^2 ('ASV HG'), 1.3 Btu/hr-ft^2 ('PCM'), 1.6 Btu/hr-ft^2 ('PCM ASV'), 0.7 Btu/hr-ft^2 ('Poly PV') and 3.9 Btu/hr-ft^2 ('Shingle'). The average ceiling heat flows in the 'PCM ASV' attic were consistently higher than the 'PCM' attic. This is surprising, since the 'PCM ASV' attic showed lower attic temperatures between the hours of about 9:00 and 18:00 than the 'PCM' attic, which includes the peak attic temperature period. Similar discrepancies were observed between the 'ASV HG' and "Poly PV' attics; peak attic temperature was higher in the 'Poly PV' attic but the peak ceiling heat flux was lower. This could be the result of some uncertainty in the HFT measurements, and needs to be further investigated.

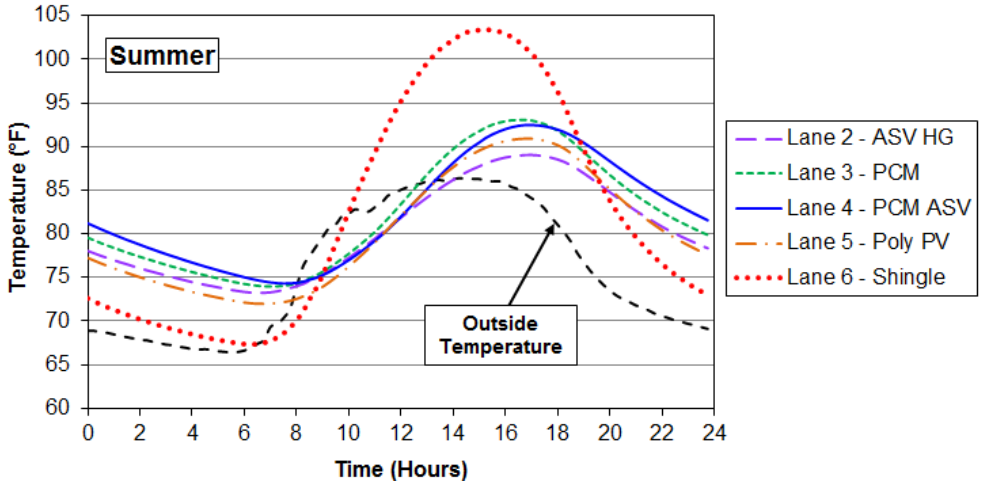

Figure 12. Bin-averaged summer attic temperatures

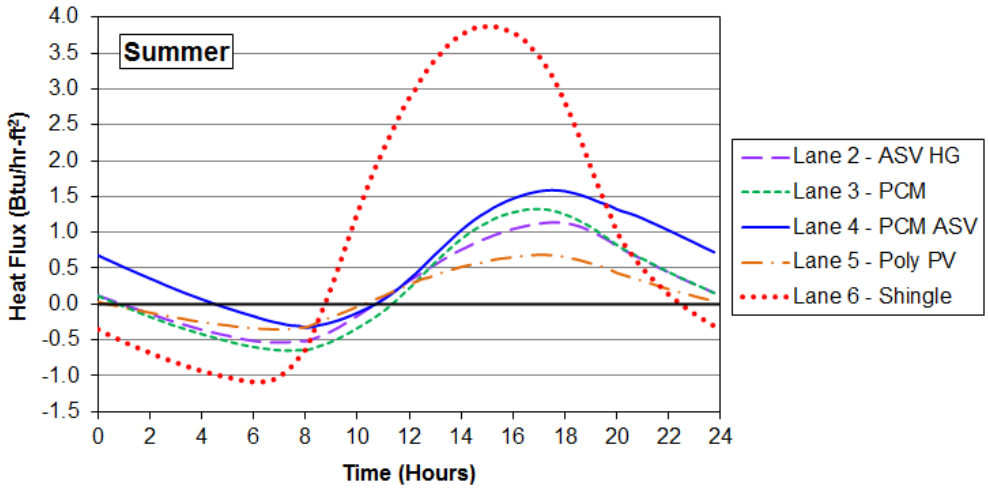

Figure 13. Bin-averaged summer ceiling heat flows

Winter Performance

Here, temperature and heat flux data from a typical winter week (December 12-18, 2012) and the overall winter period (defined as November 1, 2012 – January 1, 2013) are shown. Figure 14 shows the weekly variation of the roof heat flux. All test roofs ('Lane 2 - ASV HG', 'Lane 3 - PCM', 'Lane 4 - PCM ASV' and 'Lane 5 – Poly PV') significantly reduced both the daytime heat gains and nighttime losses compared to the control asphalt shingle roof.

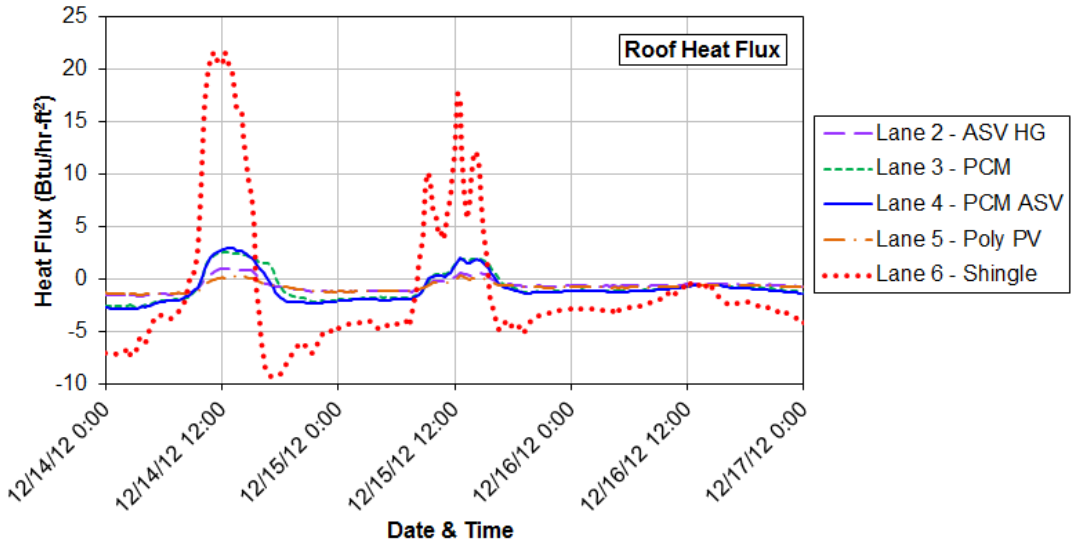

Figure 14. Winter roof heat flux variation

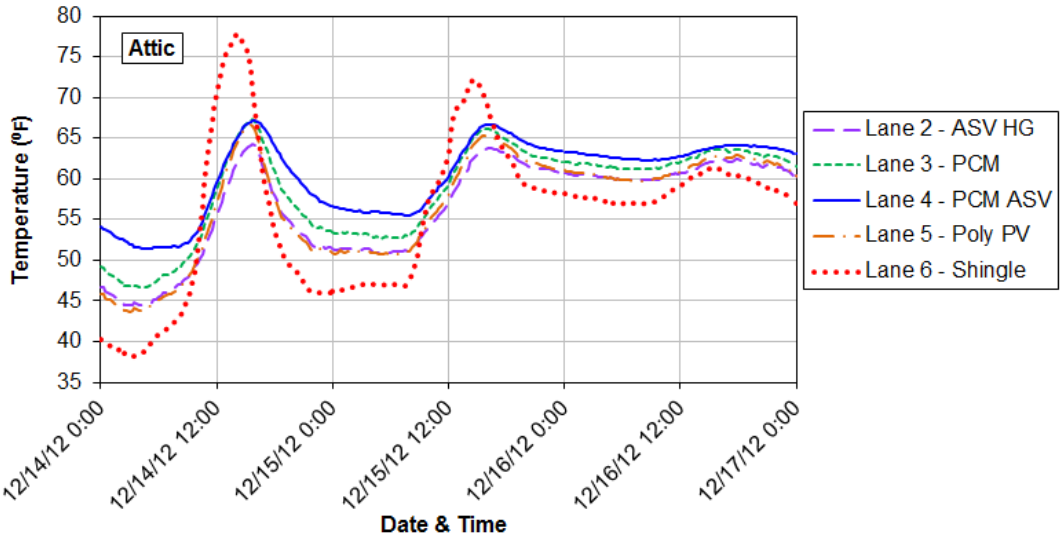

Figure 15. Winter attic temperature variation

The reductions in daytime heat gain could potentially result in a heating penalty in winter for these test roofs. However, all the attics with the dynamic test roofs remained warmer than the control attic, except during certain periods of peak solar irradiance (Figure 15). The PCM ASV roof performed the best in maintaining a warmer attic, with minimum temperatures about 11.0°F higher than the asphalt shingle attic; the minimum 'ASV HG', 'PCM', and 'Poly PV' attic temperatures were 5.6°F, 7.5°F and 5.0°F higher than the control.

Figure 16 shows the weekly ceiling heat flows during the winter week. The test roofs reduced the ceiling heat loss significantly. During this week, the heat flows were predominantly out of the conditioned space. The asphalt shingle attic added some heat to the conditioned space for brief daytime

periods. On average, the peak nighttime ceiling losses were: 'ASV HG' – 3.4 Btu/hr-ft^2, 'PCM' – 3.0 Btu/hr-ft^2, 'PCM ASV' – 2.9 Btu/hr-ft^2, 'Poly PV' – 3.5 Btu/hr-ft^2 and 'Shingle' – 4.6 Btu/hr-ft^2. Note that the negative signs have been omitted since heat loss indicates heat flow out of the conditioned space.

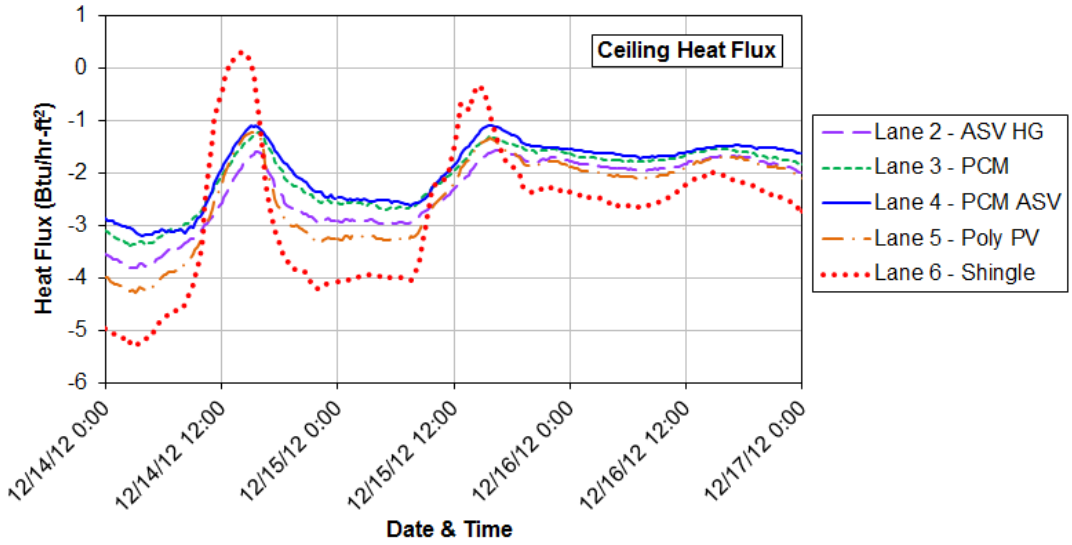

Figure 16. Winter ceiling heat flux variation

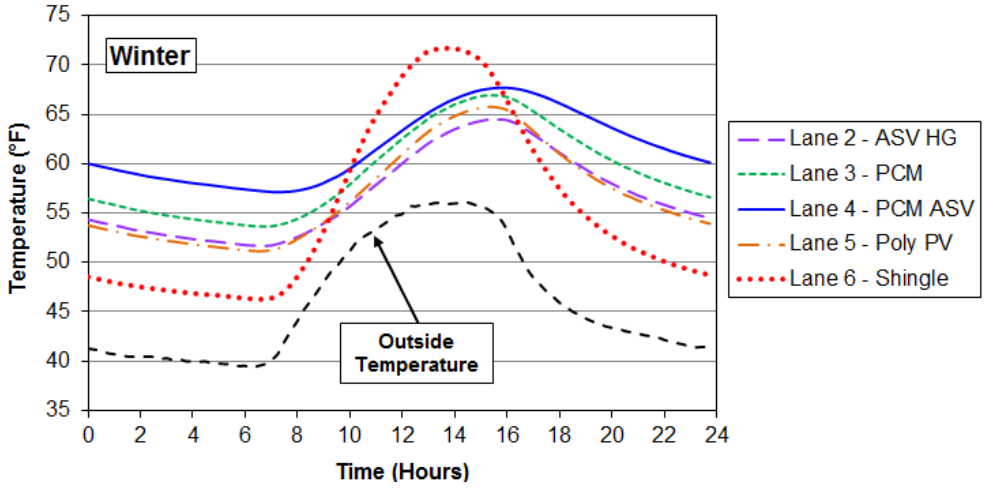

Figure 17. Bin-averaged winter attic temperatures

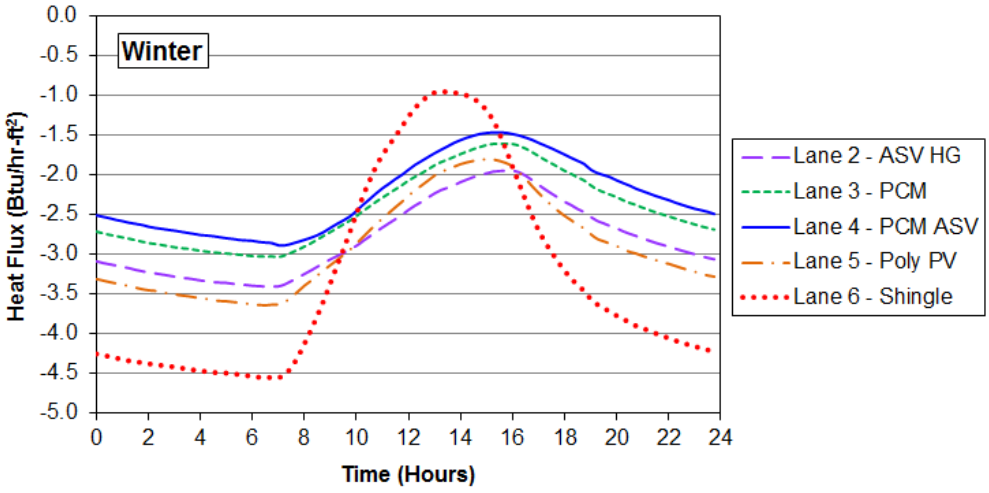

Figure 18. Bin-averaged winter ceiling heat flows

To evaluate the performance of the test roofs over the entire heating period, the bin-averaged attic temperatures and the ceiling heat flows from November 1, 2012 to January 1, 2013 are shown in Figure 17 and Figure 18. During winter, the 'PCM ASV' attic stayed warmer than both the 'ASV HG' and 'PCM' lanes. The asphalt shingle attic had warmer daytime temperatures, due to the solar heat gain, but lower nighttime temperatures than the test lanes. The minimum averaged-attic temperatures in the test lanes were 51.7°F ('ASV HG'), 53.6°F ('PCM'), 57.1°F ('PCM ASV') and 51.1°F ('Poly PV'), compared to 46.3°F in the asphalt shingle attic. The minimum ceiling heat flows (heat loss) were: -3.4 Btu/hr-ft^2 ('ASV HG'), -3.0 Btu/hr-ft^2 ('PCM'), -2.9 Btu/hr-ft^2 ('PCM ASV'), -3.6 Btu/hr-ft^2 ('Poly PV') and -4.6 Btu/hr-ft^2 ('Shingle').

PV Power Generation

The power generation of the polycrystalline solar module on lane 5 was monitored and measured using a dynamic load cell through maximum power point tracking (MPPT) technique. The load cell steps through a range of voltages and measures the resulting current, to capture the current-voltage (I-V) curve. The maximum power is obtained by electronically searching for the optimum pair current and voltage through MPPT. The maximum PV output power can be inferred from the I-V curve. More information can be found in literature from the manufacturer, Agilent.[1,2]

Figure 19 shows the typical daily power generation from the PV module on sunny days, along with the solar irradiance on the sloped PV surface. The power generation was calculated using voltage and current measured at 5-min intervals. The incident solar flux was detected using an on-site Precision Spectral Pyranometer (PSP).[3] The PSP measured the global irradiance on a surface with the same slope

[1] Agilent dc Electronic Loads, Models N3300A-N3307A, http://cp.literature.agilent.com/litweb/pdf/5980-0232E.pdf

[2] I-V Curve Characterization in High-Power Solar Cells and Modules, http://cp.literature.agilent.com/litweb/pdf/5990-4854EN.pdf

[3] Precision Spectral Pyranometer, Model PSP, http://www.eppleylab.com/

as the attic roofs. It is designed for the measurement of the total incident solar heat flux over the spectral range of 0.285 - 2.8 µm.

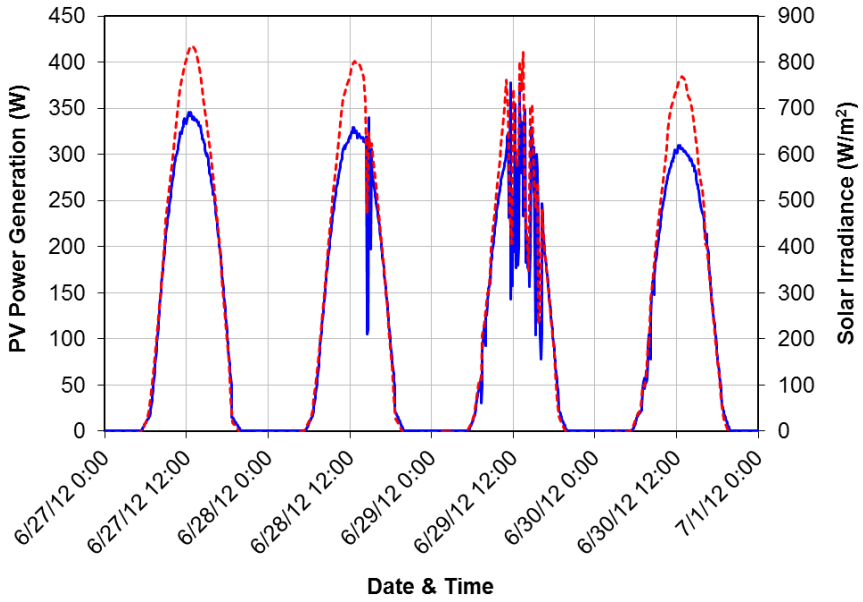

Figure 19. Sample power generation and solar irradiance on the PV module.

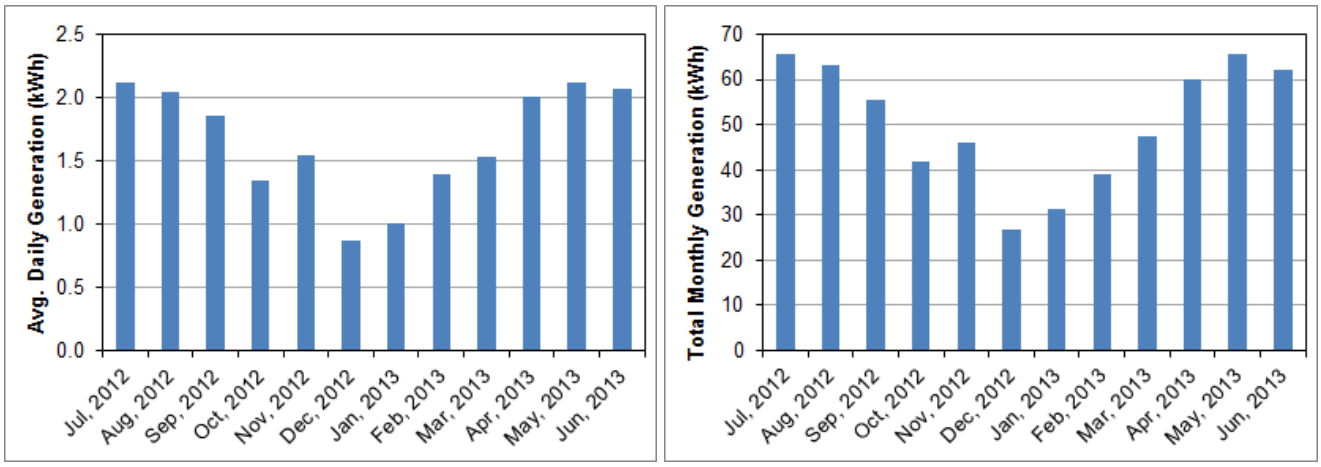

Figure 20. Average daily (left) and monthly total (right) PV energy generation.

Energy generation was calculated as: E [Wh] = P [W] x (5/60) [h]. 'E' is the energy generation over a 5 min period assuming an average power generation of 'P'. The average daily and total monthly energy generation of the PV module were calculated by integrating the 5-min energy generation over the appropriate time period, and are shown in Figure 20. It should be noted that the PV monitoring system failed for a period between Oct 20 – Nov 14, 2012. To calculate the total monthly generation, the missing data were replaced by the averaged energy generation data from the other days of the corresponding months.

CONCLUSION AND FUTURE WORK

This article presents various metal roof configurations that were tested at the ESRA facility of Oak Ridge National Laboratory during summer, fall and winter of 2012-13, and describes their potential for reducing the attic-generated space conditioning loads. These roofs contained different combinations of phase change material, rigid insulation, low emittance surface and above-sheathing ventilation, with standing-seam metal panels on top. Four test roofs were constructed and are referred to as the 'ASV HG' roof, 'PCM' roof, 'PCM ASV' roof and 'Poly PV' roof. These roofs were built on side-by-side test lanes, and compared to a control 'Shingle' roof containing asphalt shingles on OSB roof deck. All four test roofs showed the potential for substantial energy savings compared to the asphalt shingle roof. They were highly effective in reducing the heat flows through the roof and ceiling, and in reducing the diurnal attic temperature fluctuations.

The 'ASV HG' roof showed the best performance during the cooling period, while the 'PCM ASV' roof performed the best during the heating season. Attic temperatures and ceiling heat fluxes were 'bin-averaged' over summer and winter periods to compare the relative performances of the test roofs with respect to the shingle roof. During summer, the maximum attic temperatures and ceiling heat flows (peak heat gains) were compared; during winter, the minimum attic temperatures and ceiling heat flows (peak heat losses) were used for comparison. The summer and winter data are summarized in the following table:

Roof/Attic	Summer		Winter	
	Maximum attic temperature (°F)	Maximum ceiling heat flow (Btu/hr-ft^2)	Minimum attic temperature (°F)	Minimum ceiling heat flow (Btu/hr-ft^2)
Lane 2 - ASV HG	89.0	1.1	51.7	-3.4
Lane 3 - PCM	93.1	1.3	53.6	-3.0
Lane 4 - PCM ASV	92.5	1.6	57.1	-2.9
Lane 5 - Poly PV	90.9	0.7	51.1	-3.6
Lane 2 - Shingle	103.4	3.9	46.3	-4.6

Power generation of the PV module on lane 5 was monitored and measured using a maximum power-point tracking (MPPT) method. The average daily energy generation varied between 0.9 kWh during winter (Dec 2012) to 2.1 kWh during summer (Jul 2012 and May 2013).

It should be noted that the present work doesn't seek to compare metal and asphalt shingle roofs *per se*. Rather, the intent was to evaluate the energy-saving potential of roofs containing rigid insulation and dynamic features like phase change material, above-sheathing-ventilation and low-e surface with respect to a conventional shingle roof, which is the most common roof-type in the United States. The metal roofs in this study also possess different surface optical properties from shingle roofs, which also contributes to the thermal performance differences.

The data generated from these test lanes are useful in evaluating their performance in the field. However, these results are limited to the current test setup and the specific climate zone. In order to

evaluate these roofs in different climate zones and for different construction types, numerical modeling is important. The data from these tests are invaluable for validating such energy models.

ACKNOWLEDGEMENTS

The authors would like to thank Joe Harter and Derrick Fowler (ATAS International, Inc.), Sam Yuan (CertainTeed) and Pete Horvath (Phase Change Energy Solutions) for their contributions.

REFERENCES

1. Akbari, H., Berdahl, P., Levinson, R., Wiel, R., Desjarlais, A., Miller, W., Jenkins, N. Rosenfeld, A. and C. Scruton. 2004. Cool Colored Materials for Roofs. Proceedings of the ACEEE 2004 Summer Study on Energy Efficiency in Buildings. Washington, D.C.
2. Biswas, K., Miller, W., Childs, P., Kosny, J. and Kriner, S. 2011. Performance Evaluation of a Sustainable and Energy Efficient Re-Roofing Technology Using Field-Test Data. Proceedings of the 2011 NRCA International Roofing Symposium, Washington D.C., September 2011.
3. Biswas, K. and P. Childs. 2012. Performance Evaluation of Advanced Retrofit Roof Technologies Using Field-Test Data – Phase Two Final Report. ORNL/TM-2012/23. Oak Ridge, TN.
4. Castellón, C., Günther, E., Mehling, H., Hiebler, S., Cabeza, L. 2008. Determination of the enthalpy of PCM as a function of temperature using a heat-flux DSC — A study of different measurement procedures and their accuracy. International Journal of Energy Research, 32(13): 1258–1265.
5. Dodge, F.W. 2002. "Construction Outlook Forecast." www.fwdodge.com, F.W. Dodge Market Analysis Group, Lexington, MA.
6. Huang, J., Hanford, J. and F. Yang. 1999. Residential Heating and Cooling Loads Component Analysis. LBNL-44636. Berkeley, CA: Lawrence Berkeley National Laboratory.
7. Kosny, J., Biswas, K., Miller, W., Childs, P., and S. Kriner. 2011. Sustainable Retrofit of Residential Roofs Using Metal Roofing Panels, Thin-Film Photovoltaic Laminates and PCM Heat Sink Technology. Journal of Building Enclosure Design, National Institute of Building Sciences, Building Enclosure Technology and Environment Council (BETEC), Winter 2011/3.
8. Kosny J., Biswas K., Miller W., and S. Kriner. 2012. Field Thermal Performance of Naturally Ventilated Solar Roof with PCM Heat Sink. Solar Energy, 86: 2504-2514.
9. Medina, M.A. 2010. Performance of Attic Radiant Barriers (RBs) and Interior Radiation Control Coatings (IRCCs): A Summary of Published Research. Reflective Insulation Manufactures Association International – December 2010.
10. Miller, W. A. 2006. The Effects of Infrared-Blocking Pigments and Deck Venting on Stone-Coated Metal Residential Roofs. ORNL/TM-2006/9. Oak Ridge, TN.
11. Miller, W. A. and J. Kosny. 2007. Next Generation Roofs and Attics for Residential Homes. Proceedings of the 2007 ACEEE Summer Studies on Energy Efficiency, August 2007, Pebble Beach, California.

12. Parker, D., Beal, D. and S. Chandra. The Measured Summer Performance of Tile Roof Systems and Attic Ventilation Strategies in Hot, Humid Climates. Proceedings of the Thermal Performance of the Exterior Envelopes of Buildings VI, U.S. DOE/ORNL/BETEC, December 1995, Clearwater, FL.

13. Sharma, A., Tyagi, V.V., Chen, C.R., and D. Buddhi. 2009. Review on thermal energy storage with phase change materials and applications. Renewable and Sustainable Energy Reviews, 13(2): 318-345.

14. Sengoz, B. and A. Topal. 2005. Use of Asphalt Roofing Shingle Waste in HMA. Construction and Building Materials, 19(5): 337-346.

15. Xin, W., YinPing, Z., Wei, X., RuoLang, Z., QunLi, Z. and D. HongFa. 2009. Review on thermal performance of phase change energy storage building envelope. Chinese Science Bulletin, 54(6): 920-928.

16. Zalba, B., Marin, J.M., Cabeza, L.F. and H. Mehling. 2003. Review on thermal energy storage with phase change: materials, heat transfer analysis and applications. Applied Thermal Engineering, 23: 251-283.